Published by JScE as Proceedings of 4th International Conference on Earthquake Engineering and Post-Disaster Reconstruction Planning (ICEE-PDRP), 19-21 Jan. 2026, Bhaktapur, Nepal

ASSESSING SEISMIC RESPONSE IN DUAL TOWER CONNECTED STRUCTURES AT DIFFERENT STOREY LEVELS THROUGH FIXED AND FLEXIBLE CONNECTIONS

Subhekshya Shrestha[1]*, Janak Bhatta[2], Kshitiz Shrestha[1]

[1] Department of Structural Engineering, Kathmandu University
[2] Department of Earthquake Engineering, Tribhuvan University

Abstract

Skybridges are horizontal connectors between towers, influencing structural dynamics by enhancing coupling and altering dynamic load responses. This study examines seismic performance of dual eight storey tower buildings interconnected by 8 m × 14 m skybridges at three levels (first and second, third and fourth, and seventh and eighth floors). The passive isolations systems using Lead Rubber Bearings (LRB) and High Damping Rubber Bearings (HDRB) are compared with conventional rigid connections. Nonlinear time history analyses are conducted in ETABs v20.1 using matched spectral records of the New Zealand-2021 and Loma Prieta-1989 earthquakes, based on Nepal's building code NBC 105:2020 design response spectrum (475-year return period), and unscaled Gorkha-2015 earthquake. Parameters such as base shear, isolator displacement, structure displacement, drift, and hysteresis energy are analyzed. Results show a 46% base shear reduction with isolated skybridges. Lower floor isolation effectively minimizes top story displacements and inter storey drifts due to improved decoupling. Upper floor isolation leads to larger isolator displacements. LRB exhibit 14% higher energy dissipation than HDRBs. Maximum utilization of HDRB occurs under high displacements within the permissible design limits. For the cyclic load and rapid force reversal, HDRB shows stable force-displacement behavior and reduced cumulative damage.

Keywords: Dual tower structures; Skybridges; Seismic isolation; Lead rubber bearings; High damping rubber bearings; Non-linear dynamic analysis

1. Introduction

Due to urbanization in city areas, high-rise buildings are built by optimizing vertical space. The vulnerabilities in construction practices, especially in unreinforced masonry (URM) and reinforced concrete (RC) structures, were exposed in Nepal. Though RC buildings have been prevalent since the 1980s, new engineering standards were introduced in 2006. 3500 buildings post-earthquake surveys conducted exposed the vulnerability of URM and rubble stone buildings, while RC buildings failed due to code incompliance.

Nepal used seismic coefficient and response spectrum methods before Gorkha earthquake (Chaulagain et al., 2017). Malla et al. (2019) conducted detailed nonlinear analyses of RC buildings, which showed acceptable performance under 0.16g Gorkha earthquake acceleration. The inter-story drift exceeded maximum considered limit. Spectrum-compatible artificial acceleration histories were developed for Nepal, considering 23 seismic sources (Chaulagain et al., 2015). Revised Nepal Building Code 105:2020 (NBC, 2020) updated seismic hazard levels, specifying peak ground acceleration of 0.9g for critical infrastructure (Maharjan et al., 2023; Chamlagain et al., 2020).

In modern architecture, interconnected dual-tower high-rise linked by skybridges is in practice, featuring aesthetic and functionality, and also as an emergency evacuation. Complex dynamic behavior is observed in skybridges, creating dynamic coupling and altering seismic responses. The Petronas Towers in Kuala Lumpur is a double-deck flexible skybridge between the towers (Thornton et al., 1997) The 9/11 tragedy emphasized the

*Corresponding author: Subhekshya Shrestha
Department of Structural Engineering, Kathmandu University
Email: suveksa.shrestha@gmail.com
https://doi.org/10.3126/jsce.v13i1.89451

significance of such features (Wood et al., 2004). Studies show rigid connections increase internal forces, with flexible connections reducing internal forces and reduce collision risks (Wood et al., 2004; Mahmoud, 2019; Sun et al., 2011; Guo et al., 2019; Sun et al., 2011; Wu et al., 2018; Lu et al., 2018).

Experimental studies have validated the effectiveness of isolators in connected tower bridge systems. Guo, Zhou, and Lu performed shaking table tests on scaled models to evaluate isolators' performance on tower connected skybridge under PGAs of up to 0.175g. Studies on steel truss skybridges showed resilience during frequent earthquakes and collapse in rare earthquakes (Zhou et al., 2009). The research by Peng, Hussain, and Mahmoud demonstrated that dual tower frame shear wall systems with isolator link connectors effectively reduced inter-story displacement and internal forces (Peng et al., 2023; Hussain et al., 2021).

Despite these advancements in the world, Nepal's building codes lack adequate research and provisions for energy dissipating devices, seismic bracings, tuned mass dampers, and isolation systems, limiting cost-effective solutions. This study bridges this gap by evaluating the performance of Lead Rubber Bearings (LRB) and High Damping Rubber Bearings (HDRB) in high-rise dual tower structures interconnected by bridges. It uses nonlinear time history records to develop a systematic approach for their impact on seismic performance, sway, inter-storey drift, and displacement control. The research aspires to support high- rise architecture's resilience and efficient high-rise construction in seismically active regions

2. Analytical Modelling

Analytical models of two towers with one basement, ground, and seven floors each, with typical plan areas of 325.4 m^2 and 335.91 m^2 separated by 14 meters, are modeled in ETABS. External and internal wall loads of 10 kN/m and 5 kN/m respectively, are applied on beams. Floor finish, partition wall, and live loads of 1.5 kN/m^2, 1.1 kN/m^2, and 3 kN/m^2, respectively, are applied on semi-rigid diaphragm floor slabs. Skybridge slab connecting two is modelled with 25 kN/m^2 area load. Equivalent static loads are applied as user storey shear loads on diaphragms.Corbels support skybridges resting under LRB or HDRB isolators with a gap of 500 mm. A three-dimensional analytical model with an isolator link element is presented in Figure 1 and 2.

For generating the Design Based Earthquake (DBE) response spectrum, a seismic zoning factor of 0.35 for Kathmandu is adopted considering PGA for 475-year return period, and soil type "C". Importance factor is taken as 1 for class-I buildings. The normalized acceleration value of 0.875g is obtained. A ductility factor of 4 is considered for fixed base system and 2 for isolated system with drift

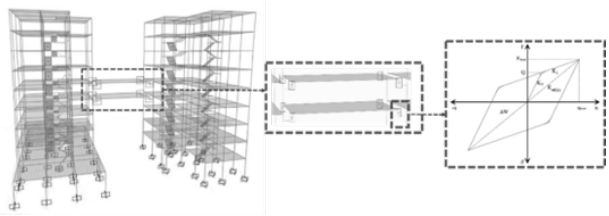

Figure 1. Three-dimensional representation of dual tower with skybridges

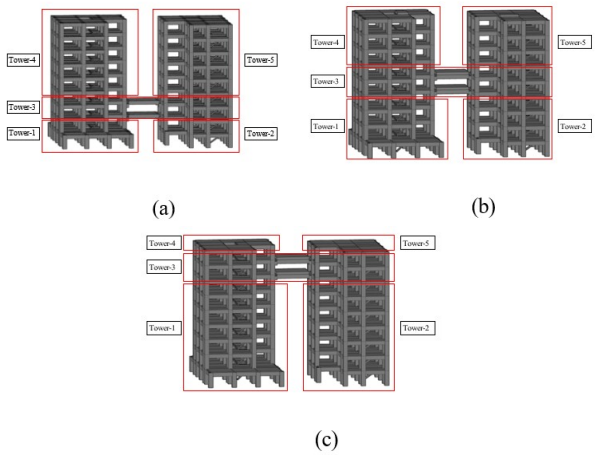

Figure 2. Three-dimensional representation of dual tower with skybridges (a) Case-I (b) Case-II (c) Case-III

limits constrained to 0.025/R and 0.02/R respectively (*UBC*, 1997 & NBC, 2020). The design response spectra are derived by reducing the spectrum by a factor of 2/3 to obtain DBE-level input. Finalized material grades and frame sizes are presented in Table 1. Skybridges are connected to towers through fixed connections or by using isolators.

Isolators are modeled as nonlinear link elements, as one elastic vertical spring and two horizontal bilinear hysteretic spring stiffness. LRB is modeled using a rubber isolator, while HDRB using plastic (Wen) with a yielding exponent of 2. Nonlinear link element behavior is illustrated in Figure 1.

The characteristic properties of LRB and HDRB are based on cross-sectional area, effective height, building period, and structural demands, following guidelines from Naeim (1999). The initial design period of 3 sec is assumed reflecting the fixed base structural period and seismic mass. Consequently, isolators with an outer diameter of 850 mm were selected. The detailed input parameters are shown in Table 2 (Bridgestone Corporation, 2017).

2.1. Time History Analysis

Three ground motions—Loma Prieta (1989), Gorkha (2015), and New Zealand (2021) with two horizontal and one vertical component each, were used for nonlinear

Table 1. Structural material and dimension specifications

Structural Design Details						
Material	Columns		Beams		Other	
	Type	Size (mm)	Type	Size (mm)	Component	Dimension
Concrete: M25	Typical	900×900	Typical	500×700	Slab thickness	150
Steel: Fe500	Skybridge	1100×1100	Skybridge	700×1600	Skybridge	14 m ×8 m
					Corbel	600 ×900
Note: All dimensions in mm unless specified otherwise.						

Table 2. Design parameters and catalogue specifications for seismic isolators

Seismic Isolator Design and Specifications				
Parameters	Symbol	Cases / Type		
		Case-I	Case-II	Case-III
Design Parameters				
Shear strain	γ	1 (100%)	1 (100%)	1 (100%)
Shear Modulus (MPa)	G	0.4	0.4	0.4
Design time period (s)	T	1.66	1.71	1.84
Damping (%)	β	5	5	5
Design accln normalized with PGA	S_a/g	0.233	0.233	0.233
Design displacement (mm)	D_d	96	99	107
Load on isolator (kN)	W	2000	2000	2000
Effective stiffness (kN/m)	k_{eff}	2917.86	2749.72	2374.90
Characteristic strength (kN)	Q	22.03	21.39	19.88
Yield displacement (mm)	D_y	0.91	0.94	1.01
Recalculated characteristic strength (kN)	Q_r	22.24	21.60	20.07
Rubber yield strength (MPa)	R_y	10	10	10
Revised rubber stiffness (kN/m)	k^*_{eff}	2686.50	2531.69	2186.59
Reduced diameter (mm)	ξ	850	837	804
Bridgestone Catalogue		**LRB**	**HDRB**	
Chosen product		LH085G4	HH085X4S	
Outer diameter (mm)		850	850	
Lead Plug diameter (mm)		120	NA	
Total rubber thickness (mm)		200	200	
Total height (mm)	H	413.1	413.1	
Linear Effective stiffness (kN/m)	$K_{eff,r}$	1560	1110	
Non-linear horizontal stiffness (kN/m)	K_h	14400	6600	
Vertical stiffness (kN/m)	K_v	3360000	3420000	
Yield strength (kN)	Q	90.1	90.7	
Post-yield ratio		0.1	0.1	
Damping (%)	β	17.8	24	
Yielding exponent		NA	2	

dynamic analysis (Figure 3, 4, 5, and Table 3). Nonlinear static analysis was first conducted for gravity and live loads, followed by fast nonlinear modal analysis to capture isolator behavior under transient vertical acceleration using a ramp function. A modal cutoff frequency filtered out non-participating mass.

The records were spectrally matched to the 5% damped DBE spectrum from NBC 105:2020 using SeismoMatch. Horizontal components were scaled using the geometric mean spectrum over periods covering 90% mass participation, with scale factors up to 3.5. Vertical scaling followed Tremblay et al. (2015), based on the vertical spectrum and peak horizontal period.

All components were applied simultaneously along principal axes. An initial scale factor of 1635 was computed from gravitational acceleration divided by ductility and overstrength factors. Peak structural responses were taken as maxima from the three nonlinear time histories per *Eurocode 1: Actions on structures* (2006). Unmatched data are shown in Figure 3, 4, and 5.

Table 3. Earthquake records with corresponding seismic parameters

Earthquake Records					
Earthquake (record)	Date	Station	PGA (g)	Mw	D_{ss} (km)
Loma Prieta	1989	Corralitos	0.63	7.0	2.8
Gorkha	2015	Kirtipur	0.26	7.8	75.7
New Zealand	2021	Raoul Island	0.80	8.1	83

PGA = Peak Ground Acceleration; Mw = Moment Magnitude; Dss = Site-source Distance

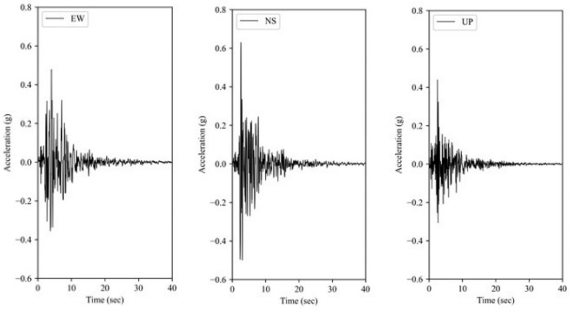

Figure 3. Time history graph for Loma Prieta earthquake:1989 (a) EW (b) NS (c) UpT

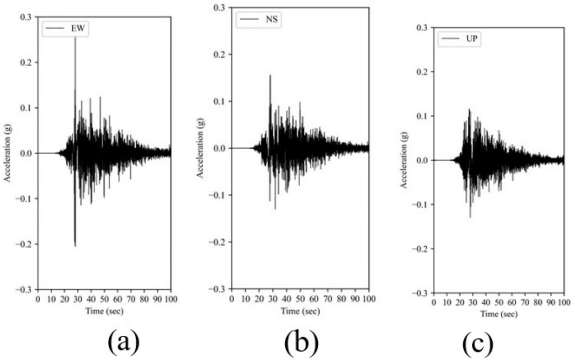

Figure 4. Time history graph for Gorkha earthquake:2015(a) EW (b) NS (c) Up

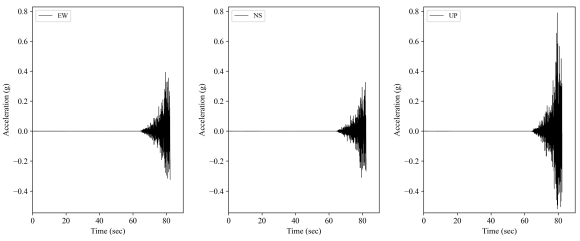

Figure 5. Time history graph for New Zealand earthquake:2021 (a) EW (b) NS (c) Up

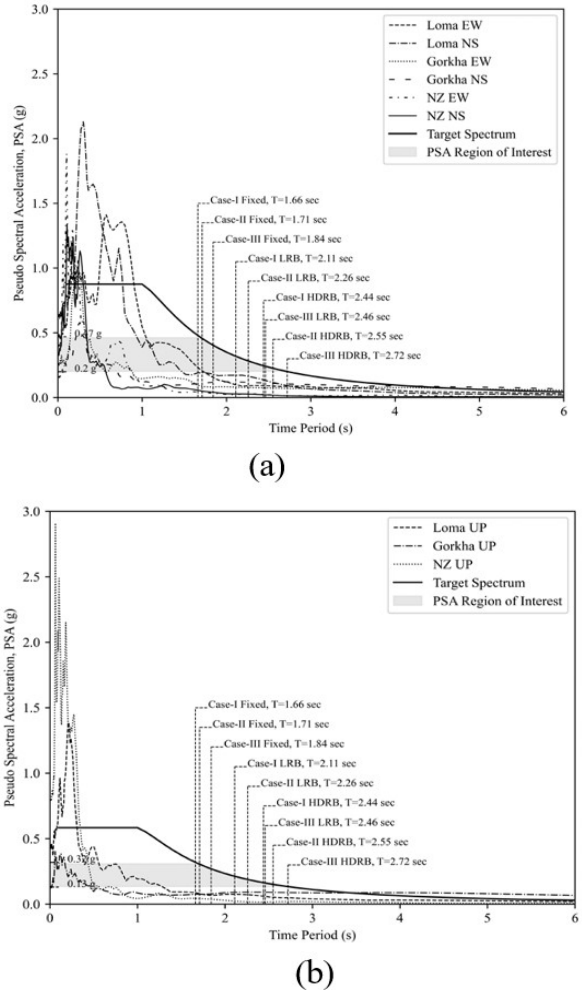

Figure 6. Comparison on response spectra and time history of selected ground motions (a) Horizontal (b) Vertical

3. Output

3.1. Base Shear

Base shear represents lateral seismic forces on the structure. The results show a clear reduction in base shear with the use of isolators compared to rigidly connected skybridge across all cases. In the X direction, Case I shows a reduction from 16,801 kN(rigid) to 15,172 kN with LRB (9.7%) and to 13,408 kN with HDRB(20.2%). In Case II, base shear reduces from 18,668 kN to 14,814 kN (20.6%) with LRB and 12,436 kN (33.3%) with HDRB. In Case III, the highest base shear(21,429 kN) occurs due to increased mode participation, but LRB and HDRB reduce this by 31.5% and 40.2% respectively. Overall, HDRBs outperform

LRBs, achieving reductions of 20.2% to 40.2%, attributed to their lower yield stiffness and higher damping. However, LRB show reduction ranging from 9.7% to 35.2%. The Y direction exhibits greater base shear reductions due to effective decoupling of lateral forces. Graphical results are presented in Table 4 and visualized in Figure 7.

Table 4. Average reduction of base shear (by percentage) in comparison with fixed systems

System	LRB		HDRB	
Direction	X	Y	X	Y
Case-I	9.7	11.6	20.2	21.3
Case-II	20.6	23.7	33.3	32.7
Case-III	31.5	35.2	40.2	39.9

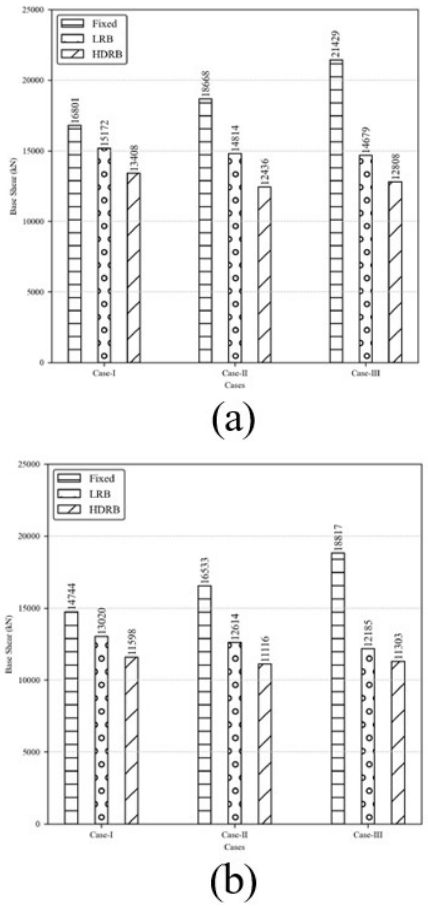

Figure 7. Base shear variation for all three cases (a) Along X direction (b) Along Y direction

3.2. Modal Mass Participation

The dynamic response is influenced by modal mass participation. In case I (rigid connection), 71.20% and 8 % of mass participate in the first and second modes respectively. Reduction in first-mode participation to 23.11%, and HDRBs further to 15.65%, effectively decouples the lateral response. Case II shows 76.32% and 24.9% for rigid, decreasing to 31.19% and 28.7% for LRB and 22.18% and 19.85% (HDRB), reflecting moderate isolation. Case III's rigid connection exhibit up to 75% participation in both modes, which drops to 32% and 23%(LRB), and 25% and 24% (HDRB) with isolation. Lower modal participation correlates with reduced base shear and increased energy dissipation, particularly for high-level skybridges (Table 5).

3.3. Top Storey Displacement

Isolator mechanical properties-yield stiffness, post-yield stiffness ratio, yield strength and damping significantly affect the dynamic response of dual-tower systems (Figure 8, Table 6). In Case I, LRBs yield a minimal 4 mm displacement reduction due to high initial stiffness, while HDRBs reduce displacement to 123mm through superior energy dissipation. In Case II, LRBs slightly increase displacement (+14mm), whereas HDRBs maintain decreased displacement (-1mm).In Case III, HDRBs outperforms LRBs with a 31mm reduction as compared to 7 mm, showing better adaptability at higher elevations. For skybridges perpendicular to towers, displacement increased for rigid connections, LRBs reduce it by 12.9% to 157mm, HDRBs by 28.3% to 129mm in Case I. In Cases II and III,HDRBs provide greater displacement control, as shown in Figure 8 and summarized in Table 6, showing superior damping and seismic performance

3.4. Joint Displacement

Figure 9 highlights the influence of the isolator's post-yield stiffness in horizontal displacements. With a post-yield ratio of 0.1, peak displacements reach 267mm(Y) and 253mm(X) in Case III.

In Case I, HDRBs reduce Y-direction displacement by 18% to LRBs but slight increment in X direction (+6.6% over LRB). In Case II, HDRBs limit X-direction displacement by 17.2% compared to LRBs, and reduce Y direction displacement more effectively. In Case III, HDRBs significantly outperform LRBs. Limiting displacement increases to 15.6% (X) and 25.8% (Y), versus 45.7% and 58.3% for LRBs. Overall, HDRBs show better control of lateral movement due to earlier energy dissipation and superior damping as presented in Table 7. Lower initial stiffness allows HDRB systems dissipate energy beforehand the global impact comes into play, reducing larger displacements. Once the initial energy is absorbed, HDRBs' damping properties dominates, effectively controlling and reducing further displacement compared to LRBs as shown in Figure 9b.

Table 5. Modal mass participation

Models												
Mode	First mode participation						Second mode participation					
System	Fixed		LRB		HDRB		Fixed		LRB		HDRB	
Direction	X	Y	X	Y	X	Y	X	Y	X	Y	X	Y
Case-I	0.0011	0.7120	0.0021	0.2311	0.0013	0.1565	0.0832	0.0011	0.0000	0.0044	0.0000	0.0043
Case-II	0.0019	0.7632	0.0065	0.3119	0.0049	0.2218	0.2493	0.0010	0.2871	0.0093	0.1985	0.0057
Case-III	0.0022	0.7537	0.0093	0.3252	0.0077	0.2536	0.7533	0.0022	0.3271	0.0146	0.2372	0.0101

Table 6. Average reduction of top floor displacement (by percentage) with fixed systems

Case	LRB				HDRB			
	X		Y		X		Y	
	Max	Min	Max	Min	Max	Min	Max	Min
I	2.7	2.8	12.9	16.6	17.7	14.0	28.3	30.9
II	-7.7	-10.0	23.4	14.9	0.7	0.7	27.5	26.1
III	4.0	0.6	26.9	6.3	17.6	7.9	34.8	14.9

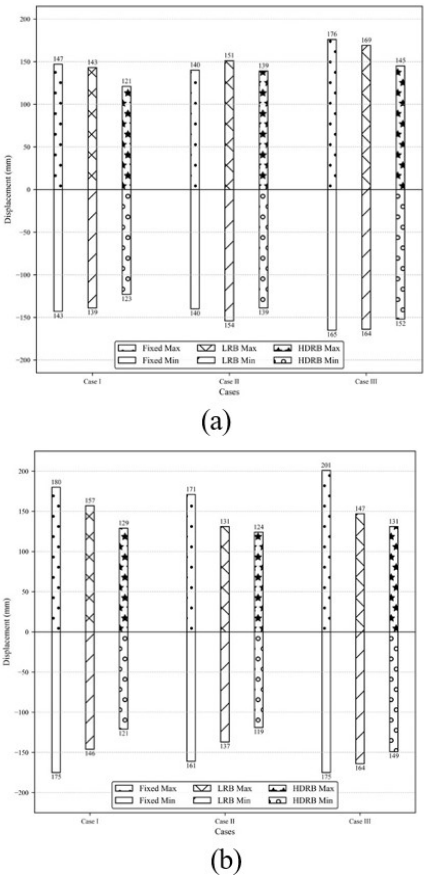

(a)

(b)

Figure 8. Variation in top storey displacement for all three cases (a)Along X direction earthquake (b) Along Y direction earthquake

3.5. Isolator to Fixed System Joint Vertical Displacement

Isolator flexibility in terms of vertical displacement ratios (isolated to fixed) decreases as skybridge height increases: 5.54 in Case-I, dropping to 2.73 in Case II as shown in Table 8. Higher ratios at lower skybridge levels indicate greater vertical movement, which benefit structures needing vertical flexibility for lesser seismic amplification but can risk isolator instability in tall buildings. HDRBs generally show slightly lower ratios. Positioning the skybridge higher, as in Case II, reduces vertical displacements in both LRB and HDRB systems, increasing overall stability.

3.6. Variation of Storey Drift

Drift is highest in fixed systems, especially in Case III. In Case I, LRBs reduce Y-direction drift by 4– 6% but increase X-direction drift by 12%, while HDRBs reduce drift by 21% (Y) and up to 14% (X). For Case II, LRBs reduce Y-direction drift by 23% but increase X-direction drift by 11%; HDRBs reduce Y drift by 27% with negligible change in X. In Case III, LRBs reduce drift by 26% (Y) and 13% (X), while HDRBs achieve the highest reductions: 33% (Y) and 24% (X). Overall, HDRBs consistently provide greater and more uniform drift control, particularly in the Y direction, minimizing torsional effects and localized stresses. Fixed systems exceed NBC drift limits in some areas, whereas isolators keep drift within UBC limits. Full results are in Figure 10 and Table 9.

3.7. Hysteresis Energy

Variation in isolator force, displacement, energy dissipation, and cycle count is shown in Table 10 and 11. In Case I, HDRB shows a higher link displacement (66 mm) than LRB (56 mm), while Case- III shows the opposite trend. At a force of 230 kN, HDRB dissipates more energy effectively with minimal damage. LRB has fewer cycles but higher energy to displacement ratio (EDR: 526 J/mm vs. HDRB's 345 J/mm). HDRB achieves higher energy to cycle ratio (ECR), especially in Case III (14659 J/cycle vs. LRB's 17521 J/cycle), indicating better energy balance. Overall, HDRB shows higher dissipation efficiency; LRB provides better energy transmission. HDRB has higher ECR and LRB has higher EDR.

4. Conclusion

The HDRB isolator outperforms LRB in energy dissipation, displacement and reducing base shear,

Table 7. Isolator to fixed system joint horizontal displacement ratio

System	LRB				HDRB			
Direction	X		Y		X		Y	
Values	Max	Min	Max	Min	Max	Min	Max	Min
Case-I	1.35	1.49	1.85	2.15	1.64	1.64	1.76	1.95
Case-II	1.80	1.47	1.89	2.05	1.23	1.57	1.49	1.87
Case-III	1.07	1.64	1.18	1.66	1.09	1.30	1.13	1.32

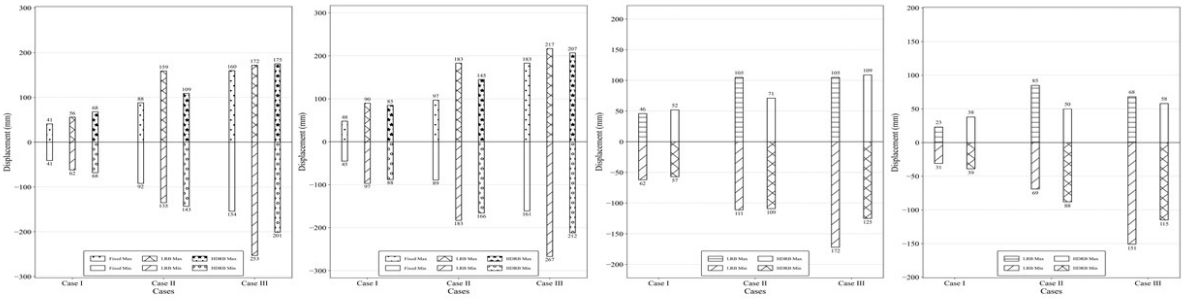

(a) (b)

Figure 9. Variation in displacement along both directions (a)Joint displacement (b) Isolator displacement

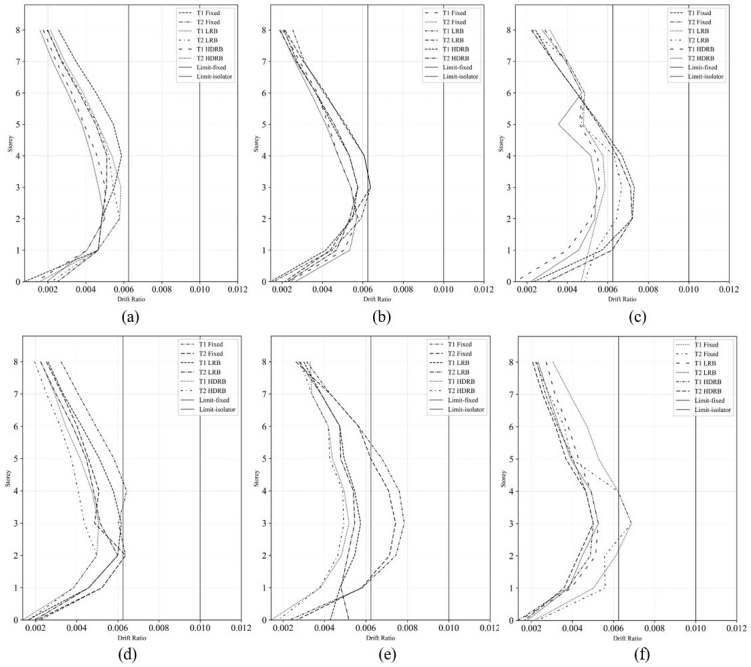

Figure 10. Variation of storey drift (a) Case-I:X (b) Case-II:X (c) Case-III:X (d) Case-I:Y (e) Case-II:Y (f) Case-III:Y

Table 8. Isolator to fixed system joint vertical displacement ratio

Case	Case-I		Case-II		Case-III	
System	LRB	HDRB	LRB	HDRB	LRB	HDRB
Value	5.54	5.25	3.77	3.68	2.73	2.70

especially for skybridge connections. HDRB provide stable top storey displacement, and mitigate high lateral forces due to high damping and lower yield stiffness. Fixed connections increased base shear and displacement, emphasizing the importance of flexible isolation systems in structural resilience. HDRB systems is effective in altering dynamic responses at greater heights, making it an optimal solution for high rise building connection in seismic region like Nepal.

The study considers isolators' nonlinearity and does

Table 9. Variation of storey drift

System	Fixed				LRB				HDRB			
Direction	X		Y		X		Y		X		Y	
Tower	T1	T2	T1	T2	T1	T2	T1	T2	T1	T2	T1	T2
Case-I	5.88	5.11	6.43	6.37	5.84	5.77	6.17	5.99	5.02	4.99	5.07	4.98
Case-II	5.76	5.70	6.87	6.87	6.38	6.38	5.26	5.26	5.75	5.75	5.01	5.01
Case-III	7.30	7.19	7.84	7.42	5.87	6.68	5.75	5.47	5.59	5.46	5.19	4.94

Table 10. Hysteresis parameters between LRB and HDRB systems in X direction

	X LRB						X HDRB					
Case	Cycle	Disp	Force	Energy	ECR	EDR	Cycle	Disp	Force	Energy	ECR	EDR
Case-I	5	56	83	29453	5891	526	12	66	103	22793	1899	345
Case-II	12	156	237	183533	15294	1176	14	150	139	139426	9959	930
Case-III	15	266	373	262820	17521	988	15	227	230	219890	14659	969

Table 11. Hysteresis parameters between LRB and HDRB systems in Y direction

	Y LRB						Y HDRB					
Case	Cycle	Disp	Force	Energy	ECR	EDR	Cycle	Disp	Force	Energy	ECR	EDR
Case-I	19	84	182	51804	2727	617	12	57	119	24780	2065	435
Case-II	15	158	221	156208	10414	989	18	147	121	118314	6573	805
Case-III	19	205	350	199135	10481	971	12	180	141	189862	15822	1055

Units: Displacement(Disp)=mm; Force=kN; Energy=J; Energy cycle ratio(ECR)=J/cycle; Energy displacement ratio(EDR)=J/mm

not incorporate structural hinge behavior, overestimating performance. Further, studies may incorporate the hinge behavior of structural elements, which may illustrate isolator effectiveness as a whole.

References

Bridgestone Corporation. (2017). *Bridgestone seismic isolation product line-up*. Bridgestone Corporation. Tokyo, Japan.

Chamlagain, D., Niraula, G., Maskey, P., Bista, M., Tamrakar, M., Gautam, B., Ojha, S., Acharya, I., & Dhakal, R. (2020). Probabilistic seismic hazard assessment of nepal for revision of national building code nbc 105 [Advance online publication]. *Journal of Earthquake Engineering*.

Chaulagain, H., Rodrigues, H., Silva, V., Spacone, E., & Varum, H. (2015). Seismic risk assessment and hazard mapping in nepal. *Natural Hazards*, *78*, 583–602.

Chaulagain, H., Rodrigues, H., Varum, H., Silva, V., & Gautam, D. (2017). Generation of spectrum-compatible acceleration time history for nepal. *Comptes Rendus Géoscience*, *349*(5), 198–201.

Eurocode 1: Actions on structures. (2006). British Standards Institution. London, United Kingdom.

Guo, W., Zhai, Z., Wang, H., Liu, Q., Xu, K., & Yu, Z. (2019). Shaking table test and numerical analysis of an asymmetrical twin-tower super high-rise building connected with long-span steel truss. *The Structural Design of Tall and Special Buildings*, *28*(13), e1630.

Hussain, S., Azeem, M., & Minhajuddin, A. (2021). Effect on seismic behaviour of structurally connected tall buildings. *International Journal of Advanced Research in Engineering and Technology*, *12*(3), 104–115.

Lu, X., Lu, Q., Lu, W., Zhou, Y., & Zhao, B. (2018). Shaking table test of a four-tower high-rise connected with an isolated sky corridor. *Structural Control and Health Monitoring*, *25*(3), e2109.

Maharjan, S., Poujol, A., Martin, C., Ameri, G., Baumont, D., Hashemi, K., Benjelloun, Y., & Shible, H. (2023). New probabilistic seismic hazard model for nepal himalayas by integrating distributed seismicity and major thrust faults. *Geosciences*, *13*(9), 220.

Mahmoud, S. (2019). Horizontally connected high-rise buildings under earthquake loadings. *Ain Shams Engineering Journal*, *10*(1), 227–241.

Malla, S., Karanjit, S., Dangol, P., & Gautam, D. (2019). Seismic performance of high-rise condominium building during the 2015 gorkha earthquake sequence. *Buildings*, *9*(2), 36.

Naeim, F. (1999). *Design of seismic isolated structures: From theory to practice*. John Wiley & Sons.

NBC. (2020). *Nbc 105:2020 – seismic design of buildings in nepal*. Ministry of Urban Development. Kathmandu.

Peng, F., Li, J., Liu, D., Li, Z., Shan, H., Liao, G., & Lei, M. (2023). Seismic response analysis of connected dual-tower isolated structure under three-dimensional earthquakes. *Ain Shams Engineering Journal*, *14*(11), 102538.

Sun, H., Cheng, L., & Chen, S. (2011). Seismic isolation analysis on long-span platform bridge connecting twin-tower structures. *Advanced Materials Research*, *255*, 1225–1229.

Thornton, C., Hungspruke, U., & Joseph, L. (1997). Design of the world's tallest buildings—petronas twin towers at kuala lumpur city centre. *The Structural Design of Tall Buildings*, *6*(4), 245–262.

Tremblay, R., Atkinson, G., Bouaanani, N., Daneshvar, P., Léger, P., & Koboevic, S. (2015). Selection and scaling of ground motion time histories for seismic analysis using nbcc 2015. *Proceedings of the 11th Canadian Conference on Earthquake Engineering (11CCEE)*.

UBC. (1997). Whittier, CA, International Conference of Building Officials.

Wood, A., Chow, W., & McGrail, D. (2004). The skybridge as an evacuation option for tall buildings for highrise cities in the far east. *Journal of Applied Fire Science*, *13*(2), 113–124.

Wu, X., Wang, J., & Zhou, J. (2018). Seismic performance analysis of a connected multitower structure with fps and viscous damper. *Shock and Vibration*, *2018*, 1865761.

Zhou, Y., Lu, X., Lu, W., & He, Z. (2009). Shake table testing of a multi-tower connected hybrid structure. *Earthquake Engineering and Engineering Vibration*, *8*(1), 47–59.

This page is intentionally left blank.